Spectroscopy and Photodissociation of ClO

Master thesis Theoretical Chemistry

Liesbeth M. C. Janssen

January 1, 2008

Theoretical Chemistry,
Institute for Molecules and Materials,
Radboud University Nijmegen

Radboud University Nijmegen

Summary

This work gives a brief overview of the spectroscopy and photodissociation of the ClO radical. It is found that the $A\,^2\Pi \leftarrow X\,^2\Pi$ transition dominates the entire UV absorption spectrum, but the contributions from other valence states are still somewhat unclear. The $a\,^4\Sigma^-$ state, presumably located at 16 000 – 17 500 cm^{-1} above the ground state, should give rise to a very weak absorption band, but this is yet to be confirmed experimentally. The precise role of the $B\,^2\Sigma^+$ state, which lies at 31 000 – 41 000 cm^{-1} above the ground state, is also a matter of debate. Moreover, the symmetries of several Rydberg states have not been established yet. In particular the D and E states, previously identified as $^2\Sigma$ states but recently assigned to $^2\Delta$ and $^2\Pi$ symmetry, must be investigated in more detail. The exact nature of the higher G and H states also remains unclear. Furthermore, the existence of the $I\,^2\Sigma^+$ state, presumably located at $\sim$ 68 900 cm^{-1} above the ground state, is yet to be confirmed experimentally.

Photodissociation studies indicate that excitation to the continuum of the $A\,^2\Pi$ state yields predominantly Cl($^2P_{3/2}$) + O($^1D_2$) fragments. The contribution from the $B\,^2\Sigma^+$ state is not clearly established yet, but recent studies suggest that the $B\,^2\Sigma^+$ state leads to the minor Cl($^2P_{1/2}$) + O($^1D_2$) channel. At excitation wavelengths below the O($^1D_2$) threshold, the $A\,^2\Pi$ state is found to be strongly predissociated. It is still unclear, however, which repulsive states are involved in the predissociation process. Furthermore, recent experiments show that exit channel coupling plays an important role in the dynamics. These results clearly highlight the need for more accurate quantum dynamical calculations to fully elucidate the predissociation mechanism.

Contents

Chapter 1

Introduction

The ClO radical has been intensively studied over the last few decades, mainly due to its importance in atmospheric chemistry. ClO is a highly reactive species and plays a crucial role in the chlorine-induced destruction of ozone [1, 2, 3]:

$$\mathrm{Cl} + \mathrm{O_3} \rightarrow \mathrm{ClO} + \mathrm{O_2}, \tag{1.1}$$

$$\mathrm{ClO} + \mathrm{O} \rightarrow \mathrm{Cl} + \mathrm{O_2}. \tag{1.2}$$

Atomic chlorine is possibly the most efficient contributor to ozone loss, and ClO is considered as the dominant chlorine substituent in the lower and middle stratosphere [2]. Hence, a detailed understanding of ClO chemistry is critical for modeling ozone concentrations in the atmosphere. Reactive collisions between ClO and other halogen monoxides, e.g. BrO, can yield stratospheric chlorine atoms via the reaction:

$$\mathrm{ClO} + \mathrm{BrO} \rightarrow \mathrm{Br} + \mathrm{Cl} + \mathrm{O_2}, \tag{1.3}$$

which may subsequently initiate the cycle of ozone depletion in reaction (1.1). It is estimated that bimolecular reactions of halogen monoxides account for 20% – 25% of the total ozone loss in the lower stratosphere [4, 5]. Another source of atomic chlorine is ultraviolet (UV) photolysis of ClO, which is responsible for 2% – 3% of the stratospheric ozone depletion [5, 6]. The role of ClO is also important in photodissociation of $\mathrm{ClONO_2}$ and $\mathrm{Cl_2O}$, where ClO is a primary photofragment that may undergo secondary photolysis [7, 8, 9].

Numerous studies have tried to elucidate the nature of the ClO radical, both experimentally and theoretically. A wide range of spectroscopic measurements has led to a detailed characterization of the electronic structure, while recent photodissociation experiments and *ab initio* calculations have provided valuable insight into the dissociation dynamics. The present work gives a brief overview of these studies and summarizes the current knowledge on ClO spectroscopy and photodissociation. The spectroscopy is described in Chapter 2 and the photodissociation process is discussed in Chapter 3. Conclusive remarks and recommendations are given in Chapter 4.

Chapter 2

Spectroscopy of ClO

The rapid development of spectroscopic techniques in the last two decades [10] has made it possible to study open-shell species at a detailed quantum mechanical level. Numerous spectroscopic methods have been applied to the ClO system, resulting in an extensive characterization of both its valence and Rydberg states. This chapter describes the most important findings of these studies.

2.1 Valence states

Emission bands of ClO were first observed by Pannetier and Gaydon [11], who identified nineteen vibrational bands in flame emission. The first ClO absorption spectrum, shown in Fig. 2.1, was recorded by Norrish and Porter [12, 13] in one of the earliest flash photolysis experiments. Based on these results, Porter [14] proposed a vibrational assignment of the observed bands, as indicated in Fig. 2.1. Subsequent work of Durie and Ramsay [15], who measured the UV absorption spectrum at higher resolution, showed that the band structure arises from the $A\,^2\Pi$ (υ') $\leftarrow$ $X\,^2\Pi$ (υ'') transition. They also derived that the electronic configurations of the ground $X\,^2\Pi$ state and excited $A\,^2\Pi$ state are $...(7\sigma)^2(2\pi)^4(3\pi^*)^3$ and $...(7\sigma)^2(2\pi)^3(3\pi^*)^4$, respectively. Additional studies by Coxon and Ramsay [16, 17, 18] indicated that the original assignment of vibrational bands was incorrect, which shifted the labels by one quantum number of υ' (see Fig. 2.2). Moreover, the previously unobserved (0,0) and (1,0) absorption bands of the $A\,^2\Pi$ (υ') – $X\,^2\Pi$ (υ'') system were recently detected by Howie *et al.* [19], who used the fairly new technique of cavity ring-down spectroscopy. These studies, and several other reinvestigations of the UV absorption spectrum [20, 21, 22, 23], have led to a detailed knowledge of the $X\,^2\Pi$ and $A\,^2\Pi$ states, and various spectroscopic properties have been determined (see Table 2.1).

In contrast to the $X\,^2\Pi$ and $A\,^2\Pi$ states, relatively little is known about other valence states of ClO. The lowest excited state is presumably the $a\,^4\Sigma^-$ state, correlating with $\mathrm{Cl}(^2P_J)$ + $\mathrm{O}(^3P_J)$ in the atomic limit. Indirect experimental evidence for this state has been provided by Nelson *et al.* [7], who studied the photolysis of Cl_2O at 248 nm. Based on the observed energy distribution of the ClO + Cl products, they concluded that ClO was formed in an electronically excited state below the first dissociation limit. Hence, they postulated the involvement of a weakly bound $^4\Sigma^-$ state with leading electronic configuration $...(7\sigma)^2(2\pi)^4(3\pi^*)^2(8\sigma^*)^1$. They suggested that ClO $(a\,^4\Sigma^-)$ was produced by a spin-orbit induced Landau-Zener transition between

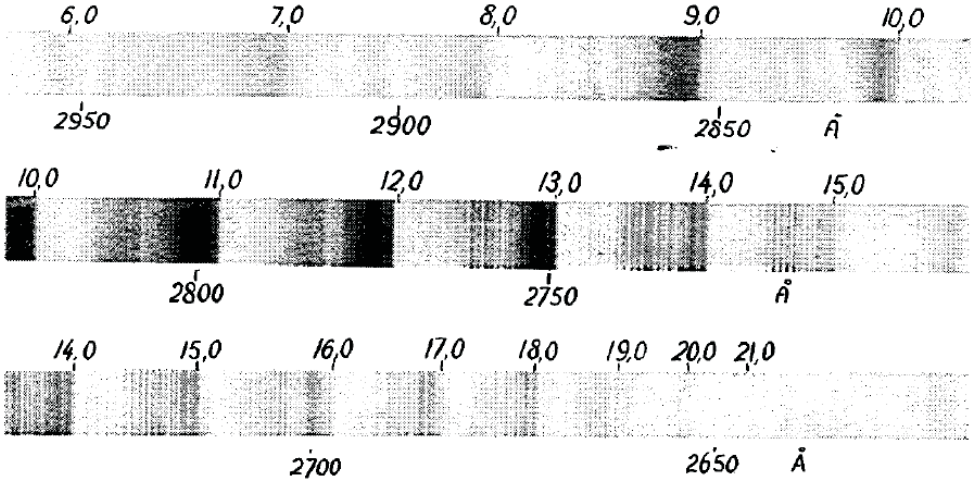

Figure 2.1: First UV absorption spectrum of ClO, measured by Norrish and Porter using flash photolysis of oxygen-chlorine mixtures. The figure is taken from Ref. [24].

a singlet and triplet surface of Cl_2O. Furthermore, they mentioned that the existence of the $a\,^4\Sigma^-$ state had been predicted by Langhoff in an unpublished *ab initio* study. Langhoff estimated that the $a\,^4\Sigma^-$ potential lies at $\sim 17\,800$ cm^{-1} above the ground state [7]. Subsequent experimental work of Nelson *et al.* [8] focused on the UV photodissociation of $ClONO_2$. They concluded that the total internal energy of the ClO + NO_2 fragments was sufficiently high to produce ClO in the $a\,^4\Sigma^-$ state, but noted that this would require a spin-forbidden transition. Moreover, they argued that ClO ($a\,^4\Sigma^-$) should easily undergo secondary photolysis, but no evidence was found for this channel. The existence of the $a\,^4\Sigma^-$ state was therefore not unequivocally confirmed in this study.

High level *ab initio* calculations by Lane *et al.* [25] and Toniolo *et al.* [26] indicated that the $a\,^4\Sigma^-$ (or $1\,^4\Sigma^-$) potential lies at 16 000 – 17 500 cm^{-1} above the ground state, with a shallow minimum at approximately 4 a_0. Toniolo *et al.* predicted that excitation to the $a\,^4\Sigma^-$ state should give a nearly continuous band in the absorption spectrum, supposedly centered around 350 nm. Although the $1\,^4\Sigma^- \leftarrow X\,^2\Pi$ transition is spin-forbidden, they argued that spin-orbit coupling between the $a\,^4\Sigma^-$ state and $A\,^2\Pi$ state gives rise to a weak oscillator strength of approximately $3 \cdot 10^{-7}$. They suggested that this transition is the only possibility to dissociate ClO at wavelengths above 320 nm, which could provide a stringent test for the location of the $a\,^4\Sigma^-$ potential.

Another low lying valence state of ClO is the $B\,^2\Sigma^+$ state, but little conclusive evidence is found regarding its nature. The existence of a $^2\Sigma^+$ state, presumably with configuration $...(7\sigma)^1(2\pi)^4(3\pi^*)^4$, was first proposed by Durie and Ramsay [15] from a consideration of possible electronic configurations. Amano *et al.* [27] estimated that this $^2\Sigma^+$ state lies at approximately 31 000 cm^{-1} above the ground state, which was based on the observed Λ-type doubling in the ClO microwave spectrum. Subsequent work of Coxon and Ramsay in the UV region [17] indicated that the $B\,^2\Sigma^+$ state is located at a slightly higher energy (35 300 cm^{-1}). Additionally, Barton *et al.* [21] reported a continuous absorption band near 270 nm, which could not be assigned to the $A\,^2\Pi \leftarrow X\,^2\Pi$ transition. These collective observations have been interpreted as indirect evidence for the existence of a $^2\Sigma^+$ state at 31 000 – 35 000 cm^{-1} [28].

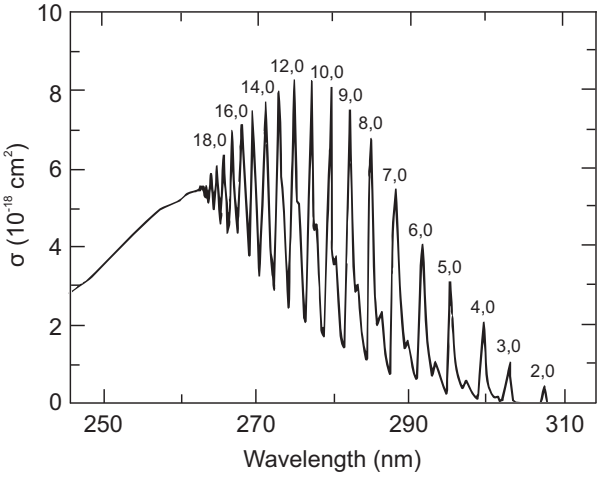

Figure 2.2: UV absorption spectrum of ClO. The figure clearly shows the progression of bands in the $A\,^2\Pi(\upsilon')$ – $X\,^2\Pi(\upsilon'')$ system. The data are adapted from Ref. [20].

Recent photodissociation studies have provided new insight into the character of the $B\,^2\Sigma^+$ state (see also Chapter 3). Davis and Lee [28] investigated the photodissociation of ClO ($\upsilon'' = 0$) at 248 nm, and concluded that a perpendicular transition contributes significantly ($\sim 30\%$) to the oscillator strength. They associated this transition with excitation to the $B\,^2\Sigma^+$ state. Furthermore, they noted that this state, when accessed at 248 nm, promptly dissociates into the atomic fragments $\mathrm{Cl}(^2P_{3/2})$ and $\mathrm{O}(^1D_2)$. *Ab initio* calculations by Lane *et al.* [25] indicated that the $B\,^2\Sigma^+$ (or $2\,^2\Sigma^+$) potential lies at $\sim 41\,000$ cm^{-1} above the ground state, and is composed of two distinct electronic configurations: $...(7\sigma)^1(2\pi)^4(3\pi^*)^4$ in the Franck-Condon region and $...(7\sigma)^2(2\pi)^3(3\pi^*)^3(8\sigma^*)^1$ at long range. They suggested that the $B\,^2\Sigma^+ \leftarrow X\,^2\Pi$ transition may carry strong oscillator strength at wavelengths shorter than 240 nm, but argued that the $B\,^2\Sigma^+$ state is inaccessible from $X\,^2\Pi$ ($\upsilon'' = 0$) at 248 nm. Other theoretical work by Toniolo *et al.* [26] showed that absorption to the $B\,^2\Sigma^+$ state only takes place in the wavelength region of 210 – 242 nm, with small oscillator strengths of approximately 2%. These results thus seem to contradict the experimental findings of Davis and Lee [28]. However, Zou *et al.* [9, 29] recently studied the UV photodissociation of jet-cooled ClO at 235 nm, and found evidence to support the conclusions of Davis and Lee. They reported that perpendicular transitions may constitute nearly one-third of the oscillator strength at 235 nm, similar to the earlier work at 248 nm. Hence, they concluded that both experimental studies were inconsistent with the results of Toniolo *et al.* [26]. Additional work by Kim *et al.* [30], who investigated ClO photodissociation in the wavelength region of 235 – 291 nm, provided new information on the role of the $B\,^2\Sigma^+$ state. They observed much smaller contributions from perpendicular transitions than previously reported by Davis and Lee and Zou *et al.*, suggesting that the $B\,^2\Sigma^+$ state is hardly involved in the $\mathrm{Cl}(^2P_{3/2})$ + $\mathrm{O}(^1D_2)$ channel. At photolysis wavelengths between 235 and 244 nm however, they found strong evidence that the minor $\mathrm{Cl}(^2P_{1/2})$ + $\mathrm{O}(^1D_2)$ channel is reached via the perpendicular $B\,^2\Sigma^+ \leftarrow X\,^2\Pi$ transition. The relative quantum yield for this channel was approximately 1%, in good agreement with the predictions of Toniolo *et al.* [26] but inconsistent with those of Lane *et al.* [25].

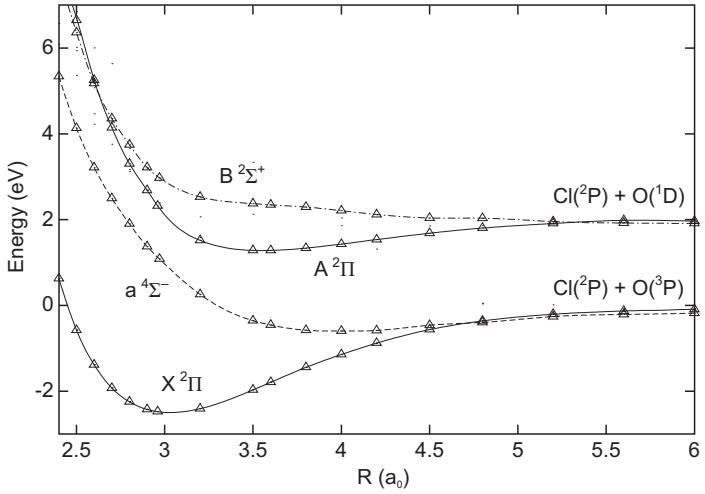

Figure 2.3: Calculated potential energy curves of the low lying valence states of ClO. The data are adapted from Ref. [26].

In conclusion, the exact nature of the $B\,^2\Sigma^+$ state has not been unambiguously established yet. Proposed values for the location of the potential vary from 31 000 to 41 000 cm^{-1} with respect to the ground state, illustrating the large discrepancy between experimental and calculated results. Another issue is whether the $B\,^2\Sigma^+$ state is effectively bound or repulsive. It has been suggested that the minimum of the potential lies below the $Cl(^2P_J) + O(^1D_2)$ dissociation limit [17, 31], implying that the $B\,^2\Sigma^+$ state is weakly bound, while theoretical studies indicate that the potential is entirely repulsive [25, 26]. Moreover, several contradictory results have been reported for the UV oscillator strength of the $B\,^2\Sigma^+ \leftarrow X\,^2\Pi$ transition, with values ranging from 1% to 30%. These discrepancies will be discussed in more detail in chapter 3.

2.2 Rydberg states

Higher excited states of ClO have been observed in vacuum-ultraviolet (VUV) absorption studies [32], VUV laser-induced fluorescence (LIF) measurements [33], and multiphoton ionization experiments [31, 34, 35, 36, 37, 38]. The first experimental evidence for these states was provided by Basco and Morse [32], who reported six Rydberg transitions in the VUV region. They noted that all Rydberg states, labeled C to H, were formed by promoting an antibonding $3\pi^*$ electron into a nonbonding Rydberg orbital. Based on the observed multiplet splittings, they concluded that the C, D, E, and F states exhibit strong $^2\Sigma$ character, while the G state is likely to have $^2\Pi$ or $^2\Delta$ symmetry. The nature of the H state could not be determined. Coxon [39] subsequently measured the $C\,^2\Sigma \leftarrow X\,^2\Pi$ absorption spectrum at high resolution, and identified the C state as a $^2\Sigma^-$ Rydberg state. Theoretical work by Wang and McKoy [40] and Lane and Orr-Ewing [41] showed that the $C\,^2\Sigma^-$ state possesses a $^3\Sigma^-$ ionic core, comparable to the electronic $X\,^3\Sigma^-$ ground state of ClO^+. These findings were confirmed by ter Steege *et al.* [31], who employed (2+1) resonance enhanced multiphoton ionization (REMPI) photoelectron spectroscopy. Based on the measured spectra, they concluded that the shape of the $C\,^2\Sigma^-$ potential strongly resembles that of the

ionic ground state, thus indicating a $^3\Sigma^-$ Rydberg core. Other experimental work by Nee and Hsu [42] and Matsumi *et al.* [33] focused on the $C\,^2\Sigma^- - X\,^2\Pi$ fluorescence spectrum, which revealed strong emission from $C\,^2\Sigma^-$ ($v' = 0$) near 170 nm. Despite favorable Franck-Condon factors, LIF signals from $v' = 1$, 2, and 3 were found to be much weaker, implying that these levels are highly predissociative [33].

(3+1) REMPI spectra via the D, E, and F states were recorded by Duignan and Hudgens [34] in the wavelength region of 420 – 474 nm. Although their results were largely consistent with those of Basco and Morse, the $F(0,0)$ bands of the VUV spectrum could not be reproduced. Hence, they proposed a reassignment of the $F\,^2\Sigma \leftarrow X\,^2\Pi$ band origin, shifting the vibrational numbering by one quantum number of v'. The $F(0,0)$ bands that were previously reported by Basco and Morse remained unassigned. A subsequent (3+1) REMPI photoelectron study by Wales *et al.* [37] confirmed the main conclusions of Duignan and Hudgens, but indicated an incorrect assignment of two $D\,^2\Sigma \leftarrow X\,^2\Pi$ transitions. Based on the photoelectron spectra, Wales *et al.* attributed these resonances to hot bands of the E state.

Despite the various REMPI studies on ClO, the symmetries of the higher Rydberg states have not been fully elucidated yet. The D, E, and F states are generally believed to be of $^2\Sigma$ symmetry [32, 34, 37], but the lack of rotational resolution has hampered a more accurate assignment [41]. In a (2+1) REMPI study by Bishenden and Donaldson [36], the symmetry label $^2\Sigma^+$ was attributed to the D, E, and F states, while Wang and McKoy [40] assumed that these states possess $^2\Sigma^-$ symmetry. It should be noted, however, that little conclusive evidence was provided to support these assignments. In an attempt to resolve the symmetries, Cooper *et al.* [38] employed (2+1) REMPI spectroscopy at 261 – 276 nm, but an accidental one-photon resonance with the $A\,^2\Pi$ state prevented excitation to higher Rydberg states. Hence, no experimental assignments could be made.

Recent theoretical work by Lane and Orr-Ewing [41] has offered new insight into the Rydberg states of ClO. High level *ab initio* calculations at the CASSCF/MRCI level of theory indicated that the D state has $^2\Delta$ symmetry, and is built upon a $^1\Delta$ ionic core with a 4sσ Rydberg orbital. The spin-orbit coupling was calculated to be 3.06 cm^{-1}, which falls within the experimental uncertainty reported by Basco and Morse [32]. It thus appears likely that the D state, previously labeled as a $^2\Sigma$ state [32], must be reassigned to $^2\Delta$ symmetry. The next Rydberg state (E) was found to converge upon the $X\,^3\Sigma^-$ core, which is consistent with the experimental results of Wales *et al.* [37]. However, Lane and Orr-Ewing showed that the Rydberg orbital has pπ symmetry instead of pσ [40], leading to the overall symmetry assignment of $E\,^2\Pi$. The calculated spin-orbit splitting for this state was 23.78 cm^{-1}, somewhat larger than the experimental error of 5 – 10 cm^{-1} [32]. Nevertheless, they argued that the next Rydberg orbital (4pσ) would lie approximately 5000 cm^{-1} higher than the 4pπ orbital, far outside the expected error of their calculations. Based on these findings, they concluded that the E state must be of $^2\Pi$ symmetry. The assignment of the F state was found to be relatively straightforward. *Ab initio* calculations showed that this state consists of a $^3\Sigma^-$ core and a 4pσ Rydberg electron, in good agreement with the work of Wales *et al.* [37]. The F state was therefore assigned to $^2\Sigma^-$ symmetry [41].

Lane and Orr-Ewing also predicted the existence of a $^2\Sigma^+$ Rydberg state, presumably located at $\sim$ 68 900 cm^{-1} above the ground state. Although no experimental

Table 2.1: Overview of the spectroscopic constants of known electronic states of ClO. T_e is the energy relative to the ground state, A is the spin-orbit constant, and ω_e and $\omega_e x_e$ are vibrational constants. All units are in cm^{-1}.

State	T_e (expt.)	T_e (theory)	A (expt.)[1]	A (theory)	ω_e	$\omega_e x_e$
$H\,^2\Delta$	74 131	73 803	⋯	⋯	1023	⋯
$G\,^2\Pi$	73 782	73 350	−35	−17.84	1066	5
$F\,^2\Sigma^-$	70 093	70 455	−4	0	981	1.4
$I\,^2\Sigma^+$	69 025[2]	68 937	−9	0	⋯	⋯
$E\,^2\Pi$	67 323	66 488	5	−23.78	1085	3.6
$D\,^2\Delta$	64 484	64 727	−7	−3.06	1052	3
$C\,^2\Sigma^-$	58 490	58 384	0	0	1077.74	6.365
$B\,^2\Sigma^+$	35 300	41 322	⋯	⋯	⋯	⋯
$A\,^2\Pi$	31 744.1	31 840.8	−521	−595	515.0	6.32
$a\,^4\Sigma^-$	⋯	17 341	⋯	⋯	324	−4.2
$X\,^2\Pi$	0	0	−321.775	−378	853.72	5.58

[1] For the Rydberg states, A is defined as the mean difference between the spin-orbit splitting of the spectra and that of the $X\,^2\Pi$ ground state [32].
[2] Mean value of the $(0,0)$ bands previously assigned to the $F\,^2\Sigma^- \leftarrow X\,^2\Pi_{3/2}$ transition.

studies have reported any REMPI transitions via this state, Duignan and Hudgens [34] noticed that two vibronic bands in the VUV spectrum, located at 68 869 and 69 181 cm^{-1}, could not be assigned. Lane and Orr-Ewing associated these bands with transitions to the $I\,^2\Sigma^+$ state. Moreover, their calculations showed that the I state has an excited $^1\Sigma^+$ core, which could explain why the $I\,^2\Sigma^+ \leftarrow X\,^2\Pi$ bands have escaped detection in previous (3+1) REMPI experiments [34, 37]. If the Rydberg state was ionized with core preservation, as observed for the G state [37], the photon energy would be insufficient to reach the $^1\Sigma^+$ state of ClO^+. Hence, (3+1) REMPI via the $I\,^2\Sigma^+$ state would be impossible [41].

In addition, Lane and Orr-Ewing attempted to resolve the symmetries of the G and H states, which have proven difficult to assign experimentally. Basco and Morse [32] reported a spin-orbit splitting of ~ 35 cm^{-1} for the G state, and therefore proposed the symmetry label of $^2\Pi$ or $^2\Delta$. Wales *et al.* [37] subsequently found that the G state converges upon a $^1\Delta$ core, but the overall symmetry assignment could not be determined. Based on electronic configuration arguments, Lane and Orr-Ewing tentatively assigned the G state to $^2\Pi$ symmetry [41]. However, the spin-orbit splitting was calculated to be 17.84 cm^{-1}, much smaller that the experimental value. They attributed this difference to inadequacies in the chosen basis set and the neglection of spin-orbit coupling with other valence states. Finally, the H state was identified as a $^2\Delta$ state, consisting of a $^3\Sigma^-$ core and a 3dδ Rydberg orbital [41]. It should be noted, however, that Lane and Orr-Ewing could not perform *ab initio* calculations on doublet states corresponding to 3dδ orbitals, and the assignment is therefore not unambiguous. Nevertheless, a rough comparison with the quartet states of ClO indicated that the $H\,^2\Delta$ state should lie ~ 500 cm^{-1} higher in energy than the G state, which is consistent with the experimental findings of Basco and Morse [32]. Table 2.1 summarizes both the calculated and experimental results for these states.

Although the work of Lane and Orr-Ewing has allowed a detailed characterization of the Rydberg states of ClO, high resolution measurements are needed to confirm the proposed reassignments. In particular the spin-orbit components of the D, E and G states must be resolved experimentally in order to validate the *ab initio* results. Furthermore, the nature of the H state still remains somewhat unclear, and both theoretical and experimental studies may be necessary to fully unravel its symmetry.

Chapter 3

Photodissociation of ClO

Photodissociation studies can reveal great insight into the nature of potential energy surfaces and the couplings between them. In principle, molecular photodissociation can proceed via two mechanisms: direct excitation to a repulsive state or indirect dissociation via a bound state that is coupled to a repulsive state (predissociation). Both mechanisms have been investigated for the ClO radical, and various experimental and theoretical studies have attempted to elucidate the photodissociation dynamics.

3.1 Photodissociation above the O($^1D_2$) threshold

The first experimental work on direct ClO photodissociation was reported by Davis and Lee [28], who studied the dissociation dynamics at 248 nm using photofragment translational energy spectroscopy. Excitation into the continuum of the $A\,^2\Pi \leftarrow X\,^2\Pi$ ($v'' = 0$) spectrum led to dominant production of Cl($^2P_{3/2}$) + O($^1D_2$) fragments ($\sim 97\%$), with a negligible yield of Cl($^2P_{1/2}$) + O($^1D_2$). The measured anisotropy parameter (β) for the Cl($^2P_{3/2}$) + O($^1D_2$) channel was found to be 1.2 ± 0.2, significantly less than the limiting value of $\beta = 2$ expected for a parallel $A\,^2\Pi \leftarrow X\,^2\Pi$ transition. They argued that the effects of saturation and parent rotation were too small to cause such a large difference in anisotropy, and hence they concluded that a perpendicular transition must be involved. As already discussed in the previous chapter, they associated this transition with the $B\,^2\Sigma^+$ state, supposedly carrying $\sim 30\%$ of the total oscillator strength. Moreover, they observed a small fraction of Cl($^2P_{1/2}$) + O(^3P_J) products, which could arise from predissociation of the $A\,^2\Pi$ state. However, the low signal intensity hindered an accurate measurement of the β parameter, and therefore the dissociation mechanism could not be resolved [28].

Schmidt *et al.* [43] studied the photodissociation of ClO at 237 – 270 nm employing (2+1) REMPI detection of O($^1D_2$). They reported a quantum yield of unity for the Cl(^2P_J) + O($^1D_2$) product channel, but could not distinguish between Cl($^2P_{3/2}$) and Cl($^2P_{1/2}$) fragments due to insufficient velocity resolution. They also determined the onset of the $A\,^2\Pi \leftarrow X\,^2\Pi$ continuum, i.e. the O($^1D_2$) threshold, to be 263.4 ± 0.2 nm. Flesch *et al.* [44] subsequently measured the O($^1D_2$) threshold at higher resolution using single-photon ionization, and obtained a value of 263.71 ± 0.01 nm for the $A\,^2\Pi_{3/2}$ component. The O($^1D_2$) yield below the $A\,^2\Pi_{3/2}$ threshold was estimated to be ~ 0.2, a result that was attributed to photodissociation of the $X\,^2\Pi_{1/2}$ state. Furthermore, they noted that only low lying rotational levels of the ground state lead to O($^1D_2$)

formation, suggesting that dissociation from higher rotational states is hindered by a rotational barrier [44].

Zou *et al.* [9, 29] used REMPI time-of-flight (TOF) mass spectroscopy to investigate the photodissociation dynamics of jet-cooled ClO at 235 nm. The dominant product channel ($\sim 96\%$) was found to be $\mathrm{Cl}(^2P_{3/2}) + \mathrm{O}(^1D_2)$, with a best fit anisotropy parameter of 1.2 ± 0.2. No signal was observed from $\mathrm{Cl}(^2P_{3/2})$ in coincidence with $\mathrm{O}(^3P_J)$ atoms. They concluded that the dominant $\mathrm{O}(^1D_2)$ channel is mainly reached via the $A\,^2\Pi$ state, but noted that contributions from the $B\,^2\Sigma^+$ state are non-negligible [29]. Furthermore, Zou *et al.* reported equal quantum yields for the minor $\mathrm{Cl}(^2P_{1/2}) + \mathrm{O}(^1D_2)$ and $\mathrm{Cl}(^2P_{1/2}) + \mathrm{O}(^3P_J)$ channels, both with an estimated value of 0.02 ± 0.01. The observed β parameter for the $\mathrm{Cl}(^2P_{1/2}) + \mathrm{O}(^3P_J)$ channel was found to be 1.1 ± 0.3, suggesting the involvement of a perpendicular transition. They argued that the $\mathrm{O}(^3P_J)$ product channel arises from initial excitation to the $A\,^2\Pi$ state, followed by coupling to one or more repulsive states. These states may account for the deviation from limiting parallel anisotropy. The β parameter for the $\mathrm{Cl}(^2P_{1/2}) + \mathrm{O}(^1D_2)$ channel could not be determined due to insufficient velocity resolution, although a positive anisotropy ($\beta > 0$) produced a slightly better fit to the experimental data [29].

Kim *et al.* [30] focused on the wavelength-dependent photodissociation dynamics of jet-cooled ClO at 235 – 291 nm. They employed velocity map imaging to measure the photofragment velocity distributions, and found that $\mathrm{Cl}(^2P_{3/2}) + \mathrm{O}(^1D_2)$ is the dominant channel above the $\mathrm{O}(^1D_2)$ threshold. No signal was observed from the minor $\mathrm{Cl}(^2P_{3/2}) + \mathrm{O}(^3P_J)$ channel at wavelengths below 248 nm, while the $\mathrm{Cl}(^2P_{1/2}) + \mathrm{O}(^1D_2)$ channel could not be detected at wavelengths longer than 248 nm. Moreover, they found that the total $\mathrm{Cl}(^2P_{1/2})/\mathrm{Cl}(^2P_{3/2})$ branching ratio is wavelength-independent above the $\mathrm{O}(^1D_2)$ threshold, although the relative product yields for each dissociation channel showed small variations with wavelength. These results are consistent with the work of Davis and Lee [28] and Zou *et al.* [29]. The measured anisotropy parameters, however, were significantly different from those reported in previous studies. Kim *et al.* obtained a best fit anisotropy parameter of 1.9 ± 0.1 for the dominant $\mathrm{Cl}(^2P_{3/2}) + \mathrm{O}(^1D_2)$ channel at 235 nm, suggesting that the $A\,^2\Pi$ state carries most of the oscillator strength. They argued that their previously reported non-limiting value of 1.2 ± 0.2 [29] partially arose from the large entrained atomic signal in the TOF spectra. Furthermore, they measured a best fit anisotropy parameter of -1.0 ± 0.1 for the $\mathrm{Cl}(^2P_{1/2}) + \mathrm{O}(^1D_2)$ channel, which they attributed to excitation to the $B\,^2\Sigma^+$ state. Note that Davis and Lee [28] and Zou *et al.* [29] could not determine the anisotropy of this channel due to insufficient resolution. Kim *et al.* observed a $\mathrm{Cl}(^2P_{1/2}) + \mathrm{O}(^1D_2)$ quantum yield of $\sim 1\%$, implying that the $B\,^2\Sigma^+$ state carries very little oscillator strength above the $\mathrm{O}(^1D_2)$ threshold. These findings thus contradict the conclusions of Davis and Lee [28] and Zou *et al.* [29]. Furthermore, the minor $\mathrm{Cl}(^2P_{1/2,\,3/2}) + \mathrm{O}(^3P_2)$ channels were found to exhibit a positive anisotropy at all wavelengths below 262 nm, with best fit parameters of 0.7 – 1.5 for $\mathrm{Cl}(^2P_{1/2}) + \mathrm{O}(^3P_2)$ and 0.1 – 0.2 for $\mathrm{Cl}(^2P_{3/2}) + \mathrm{O}(^3P_2)$. Similar to the earlier work of Zou *et al.* [29], they concluded that the less-than-limiting anisotropy for $\mathrm{O}(^3P_2)$ is most likely due to curve crossings between the $A\,^2\Pi$ state and one or more repulsive states. They estimated that the curve crossing probability decreases from a maximum value of 2% at 262 nm to $< 0.2\%$ at 244 nm, but the states associated with these crossings could not be identified.

Ab initio calculations by Lane *et al.* [25] and Toniolo *et al.* [26] have also provided insight into the UV photodissociation of ClO. As already mentioned in the previous chapter, these studies have reported contradicting results on the role of the $B\,^2\Sigma^+$ state. Lane *et al.* [25] showed that the $B\,^2\Sigma^+ \leftarrow X\,^2\Pi$ transition requires promotion of a single electron in the Franck-Condon region, and hence they concluded that the transition dipole moment should be quite large. Although they did not calculate the oscillator strength for this transition, they suggested that the contribution from the $B\,^2\Sigma^+$ state should be significant at wavelengths shorter than 240 nm. These findings are consistent with the experimental work of Zou *et al.* [29]. However, Davis and Lee [28] observed a large contribution from the $B\,^2\Sigma^+$ state at 248 nm, while Lane *et al.* concluded that the $B\,^2\Sigma^+$ state is inaccessible at this wavelength. They pointed out that calculations with a larger basis set could possibly lower the $B\,^2\Sigma^+$ potential, but also argued that the observed signal at 248 nm could be contaminated by contributions from the $X\,^2\Pi_{3/2}$ ($v'' = 1$) state or the $X\,^2\Pi_{1/2}$ state.

In contrast to the work of Lane *et al.*, Toniolo *et al.* [26] showed that UV photodissociation of ClO proceeds almost entirely via the $A\,^2\Pi \leftarrow X\,^2\Pi$ transition. They also calculated the oscillator strengths for several other transitions, but none of them gave significant contributions to the absorption spectrum. The strongest transition was attributed to the $B\,^2\Sigma^+$ state, with an absorption maximum at 225 nm. However, this oscillator strength was still 30 times smaller than that of the $A\,^2\Pi \leftarrow X\,^2\Pi$ transition, and thus cannot explain the non-limiting anisotropy observed by Davis and Lee [28] and Zou *et al.* [29]. The experimental results of Kim *et al.* [30] are, however, in very good agreement with the work of Toniolo *et al.* [26]. Kim *et al.* associated the $B\,^2\Sigma^+$ state with formation of $\mathrm{Cl}(^2P_{1/2}) + \mathrm{O}(^1D_2)$ fragments, and measured a relative quantum yield of approximately 1%. Based on these findings, it thus seems plausible that the $B\,^2\Sigma^+$ state is only involved in the minor $\mathrm{Cl}(^2P_{1/2}) + \mathrm{O}(^1D_2)$ channel. However, this would imply that the perpendicular behaviour observed for the dominant $\mathrm{Cl}(^2P_{3/2}) + \mathrm{O}(^1D_2)$ channel, as previously reported by Davis and Lee [28] and Zou *et al.* [29], must be entirely attributed to experimental inaccuracies.

In conclusion, the photodissociation of ClO above the $\mathrm{O}(^1D_2)$ threshold has not been fully unraveled yet. Although all experimental studies unambiguously establish that the $A\,^2\Pi \leftarrow X\,^2\Pi$ transition is dominant and yields mainly $\mathrm{Cl}(^2P_{3/2}) + \mathrm{O}(^1D_2)$ fragments, the precise role of the $B^2\Sigma^+$ state is still somewhat unclear. Several experimental studies [28, 29] suggest that the $B\,^2\Sigma^+$ state carries significant oscillator strength and promptly dissociates into $\mathrm{Cl}(^2P_{3/2}) + \mathrm{O}(^1D_2)$, while the most recent experimental study [30] shows that excitation to the $B\,^2\Sigma^+$ state leads to the minor $\mathrm{Cl}(^2P_{1/2}) + \mathrm{O}(^1D_2)$ channel. In addition, several *ab initio* studies have reported contradicting results on the role of the $B\,^2\Sigma^+$ state. It has been suggested that the $B\,^2\Sigma^+ \leftarrow X\,^2\Pi$ transition contributes significantly to the UV absorption cross section [25], while an explicit calculation of the $B\,^2\Sigma^+ \leftarrow X\,^2\Pi$ oscillator strength has shown that the $B\,^2\Sigma^+$ state is hardly involved in the dissociation process [26]. These apparent differences clearly highlight the need for further research on ClO photodissociation. It must be noted, however, that the most accurate experimental results to date, those of Kim *et al.* [30], are in good agreement with the quantitative calculations of Toniolo *et al.* [26]. Based on these two studies, it appears likely that the $B\,^2\Sigma^+$ state plays only a minor role in the dissociation dynamics. Nevertheless, given the large discrepancy with other experimental data, this matter still remains a subject of debate.

3.2 Predissociation dynamics

As already mentioned in Chapter 2, the most prominent feature of the ClO absorption spectrum is the progression of bands arising from the $A\,^2\Pi$ (v') $\leftarrow$ $X\,^2\Pi$ (v'') transition. Flash photolysis experiments by Durie and Ramsay [15] and Coxon and Ramsay [17] indicated that all $v' - 0$ subbands of the $A\,^2\Pi - X\,^2\Pi$ system are broadened by predissociation, with v'-dependent linewidths ranging from 0.3 to > 5 cm^{-1}. Bunker and Klein [45] attempted to interpret this v'-dependence in terms of a single interacting repulsive state. They found that a single dissociative curve gives a smooth variation of linewidth as a function of v', which is inconsistent with the rapid variation observed experimentally. Hence, they concluded that more than one repulsive state must be involved in the predissociation process. McLoughlin *et al.* [23] subsequently measured the ClO absorption spectrum at higher resolution, and found that high v' levels suffer less severe predissociation than low vibrational levels. Although this observation is consistent with the earlier work of Coxon and Ramsay, the estimated linewidths for the $A\,^2\Pi_{3/2}$ state were found to be 2 – 3 times larger than previously reported. McLoughlin *et al.* attributed this discrepancy to differences in the spectral resolution. Furthermore, they concluded that the efficiency of predissociation in the $A\,^2\Pi_{3/2}$ state is comparable to that in the $A\,^2\Pi_{1/2}$ component, even though the linewidths of the $A\,^2\Pi_{1/2} \leftarrow X\,^2\Pi_{1/2}$ bands could not be accurately determined. Nevertheless, they estimated that the v'-dependent lifetimes of the two spin-orbit components should differ by no more that a factor of three.

Recent experimental and theoretical studies have provided new insight into the predissociation dynamics of ClO. Howie *et al.* [19] employed cavity ring-down spectroscopy to measure the $v' - 0$ bands ($v' \leq 7$) at high rotational resolution, and confirmed that the linewidths of the $A\,^2\Pi_{3/2}$ and $A\,^2\Pi_{1/2}$ states exhibit a marked dependence on v'. However, no evidence was found for J-dependent predissociation, and hence they concluded that molecular rotation does not play a significant role in the dynamics. Based on these results, Lane *et al.* [25] attempted to elucidate the predissociation mechanism by means of high level *ab initio* calculations. They computed the potential energy curves of all low lying doublet and quartet states of ClO, and identified several states that could be involved in the predissociation process. They assumed that the most important states are those of which the electronic configuration differs by no more than one spin-orbital from the leading $A\,^2\Pi$ state configuration. These principal candidates were identified with the $1\,^4\Sigma^+$, $1\,^4\Delta$, $2\,^2\Sigma^-$, and $2\,^4\Sigma^-$ states. They also considered the repulsive $3\,^2\Pi$ state as a strong candidate, even though its dominant configuration differs by three spin-orbitals from that of the $A\,^2\Pi$ state. Nevertheless, they argued that the electrostatic interaction between the $A\,^2\Pi$ and $3\,^2\Pi$ state should be of the same order of magnitude as the spin-orbit coupling with other repulsive curves. They subsequently performed Fermi Golden Rule calculations on this limited set of potentials and compared the resulting v'-dependent linewidths to those measured by Howie *et al.* [19]. Based on this comparison, they concluded that the $1\,^4\Sigma^+$, $2\,^4\Sigma^-$, and $3\,^2\Pi$ states are the dominant states involved in the predissociation process. It must be noted, however, that the relevant coupling strengths for the different potentials were not explicitly calculated, but derived from a fit to the experimental data. Overall their simulations were in reasonably good agreement with experiment, although the linewidths of the $v' = 2$ and $v' = 7$ levels of the $A\,^2\Pi_{3/2}$ state

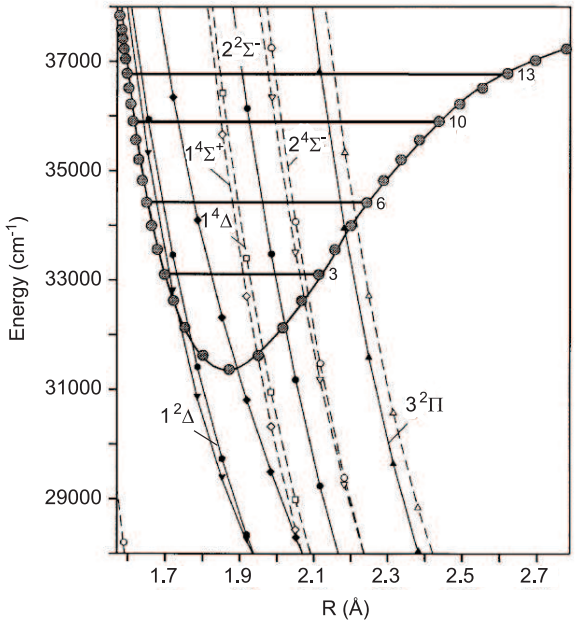

Figure 3.1: Expanded view of the Franck-Condon region of the $A\,^2\Pi$ state and the different repulsive potentials. The figure is taken from Ref. [25].

could not be reproduced. Moreover, a comparison with the work of McLoughlin *et al.* [23] revealed that the predissociation rates of the higher vibrational levels ($v' \leq 9$) were also somewhat underestimated. Lane *et al.* suggested that the $1\,^2\Delta$ state, whose minor electronic configuration differs by one spin-orbital from the dominant $A\,^2\Pi$ state configuration, could possibly account for these discrepancies. Finally, they noted that the predissociation rates for the $A\,^2\Pi_{3/2}$ and $A\,^2\Pi_{1/2}$ components exhibit a similar dependence on v', despite the marked differences in the absolute values.

Toniolo *et al.* [26] also employed high level *ab initio* calculations to study the predissociation dynamics of ClO. They calculated the spin-orbit and electrostatic couplings for several repulsive doublet and quartet states and evaluated their individual contributions as a function of v' and J. They concluded that the $3\,^2\Pi$, $1\,^2\Delta$, and $2\,^4\Sigma^-$ states are mainly responsible for predissociation of the $A\,^2\Pi_{3/2}$ state, while the $3\,^2\Pi$ and $1\,^2\Sigma^+$ states play an important role in the $A\,^2\Pi_{1/2}$ predissociation mechanism. Their calculations showed that the linewidths are largely independent of J, thus confirming the experimental results of Howie *et al.* [19]. However, the calculated v'-dependent linewidths revealed some significant discrepancies with experiment, especially at low vibrational levels. Nevertheless, the rapid variation of linewidth as a function of v' was correctly reproduced. They also found that the $A\,^2\Pi_{3/2}$ and $A\,^2\Pi_{1/2}$ components are almost equally predissociated, in good agreement with the work of McLoughlin *et al.* [23].

Kim *et al.* [30, 46] investigated the predissociation dynamics of the $A\,^2\Pi_{3/2}$ state by measuring the v'-dependent branching ratios of the $\mathrm{Cl}(^2P_J)$ + $\mathrm{O}(^3P_J)$ channels. A preliminary velocity map imaging study [30] indicated that the $\mathrm{Cl}(^2P_{3/2})/\mathrm{Cl}(^2P_{1/2})$ branching ratios for $v' = 5$ and $v' = 19$ are approximately equal (1.5 ± 0.1), but the coincident $\mathrm{O}(^3P_{2,1,0})$ state distributions were not determined. They subsequently measured the branching ratios for $v' = 6 - 11$ at the correlated state level, providing a more

detailed insight into the predissociation mechanism [46]. Their experiments showed that the correlated state distributions are highly dependent on v' but independent of J, thus confirming the earlier conclusions of Howie *et al.* [19] and Toniolo *et al.* [26]. In order to elucidate the predissociation mechanism, Kim *et al.* compared their results with the theoretical model of Lane *et al.* [25]. They evaluated the product branching ratios for the $1\,^4\Sigma^+$, $2\,^4\Sigma^-$, and $3\,^2\Pi$ states in both the diabatic and adiabatic limits, and found that the overall $\mathrm{Cl}(^2P_J)$ distributions are closely reproduced by the diabatic model. However, the branching ratios measured at the correlated level were in poor agreement with the calculated results. Kim *et al.* attempted to fit the experimental data by adjusting the relative contributions of the $1\,^4\Sigma^+$, $2\,^4\Sigma^-$, and $3\,^2\Pi$ states, but this led to only marginally better agreement. Including the $1\,^4\Delta$ and $1\,^2\Delta$ states also failed to improve the calculations. Based on this analysis, they concluded that the effects of exit channel coupling, neglected in their work, should be treated explicitly in order to accurately model the ClO predissociation dynamics.

In summary, the predissociation mechanism of the $A\,^2\Pi$ state still remains unclear. Numerous experimental studies have shown that the predissociation rates oscillate significantly as a function of v', but an accurate description of the predissociation dynamics has not been provided yet. A combined theoretical and experimental study [19, 25] indicated that the $1\,^4\Sigma^+$, $2\,^4\Sigma^-$, and $3\,^2\Pi$ states are largely responsible for predissociation of the $A\,^2\Pi_{3/2}$ and $A\,^2\Pi_{1/2}$ components, but the corresponding v'-dependent linewidths revealed some significant differences between theory and experiment. Other theoretical work [26] suggested that the $3\,^2\Pi$, $1\,^2\Delta$, and $2\,^4\Sigma^-$ states are the primary states that predissociate the $A\,^2\Pi_{3/2}$ state, while the $3\,^2\Pi$ and $1\,^2\Sigma^+$ states are dominantly involved in the $A\,^2\Pi_{1/2}$ predissociation mechanism. However, these theoretical results also failed to reproduce the experimental data. Furthermore, a recent experimental study [46] showed that the correlated branching ratios of the $\mathrm{Cl}(^2P_J)$ + $\mathrm{O}(^3P_J)$ products are in poor agreement with both the diabatic and adiabatic limits of the different repulsive potentials, illustrating the importance of exit channel coupling in the dynamics. These collective results clearly indicate that more accurate quantum dynamical calculations are needed to fully elucidate the predissociation mechanism.

Chapter 4

Conclusions and outlook

This work has provided a brief overview of the spectroscopy and photodissociation of the ClO radical. Numerous studies have shown that both the continuous and structured regions of the ClO absorption spectrum are dominated by the $A\,^2\Pi \leftarrow X\,^2\Pi$ transition, but the contributions from other valence states are still somewhat unclear. High level *ab initio* calculations have indicated that the $a\,^4\Sigma^-$ state, presumably located at 16 000 – 17 500 cm^{-1} above the ground state, gives rise to a very weak absorption band at 350 nm, but this is yet to be confirmed experimentally. It has also been suggested that the $a\,^4\Sigma^- \leftarrow X\,^2\Pi$ transition is the only possibility to photodissociate ClO at wavelengths above 320 nm, which could provide a stringent test for the location of the $a\,^4\Sigma^-$ potential.

The exact nature of the $B\,^2\Sigma^+$ state also remains unclear. Several studies have shown that this state carries significant oscillator strength in the UV region, while more recent studies indicate that the contribution from the $B\,^2\Sigma^+$ state is almost negligible. Moreover, the exact location of the $B\,^2\Sigma^+$ potential has not been established yet. Proposed values range from 31 000 to 41 000 cm^{-1} with respect to the ground state, illustrating the large discrepancy between experimental and theoretical results. An accurate measurement of this potential energy minimum could also reveal whether the $B\,^2\Sigma^+$ state is effectively bound or repulsive.

Various experimental and theoretical studies have focused on the Rydberg states of ClO, but most of these states are still not fully characterized. In particular the D and E states, previously identified as $^2\Sigma$ states, must be investigated in more detail. A recent *ab initio* study has shown that these states possess $^2\Delta$ and $^2\Pi$ symmetry, respectively, but high resolution measurements are needed to confirm the proposed reassignments. The nature of the higher G and H states also remains unclear. Furthermore, the existence of the $I\,^2\Sigma^+$ state, as predicted from *ab initio* calculations, is yet to be confirmed experimentally.

Numerous studies have established that the UV photodissociation of ClO proceeds mainly via the $A\,^2\Pi$ state, and yields primarily $Cl(^2P_{3/2})$ + $O(^1D_2)$ fragments at energies above the $O(^1D_2)$ threshold. It has been suggested that the $B\,^2\Sigma^+$ state also contributes significantly to the formation of $Cl(^2P_{3/2})$ + $O(^1D_2)$, but more recent studies indicate that the $B\,^2\Sigma^+$ state leads only to minor $Cl(^2P_{1/2})$ + $O(^1D_2)$ channel. The precise role of the $B\,^2\Sigma^+$ state is thus not fully elucidated yet. Nevertheless, based on the most accurate results to date, it appears likely that this state is only marginally involved in the photodissociation process.

The UV photodissociation of ClO below the O($^1D_2$) threshold, i.e. in the structured region of the spectrum, has also been studied extensively. It is now well established that all subbands of the $A\,^2\Pi(v') \leftarrow X\,^2\Pi(v'')$ system are broadened by predissociation, but the v'-dependent predissociation mechanism still remains unclear. It has been suggested that the repulsive $1\,^4\Sigma^+$, $2\,^4\Sigma^-$, and $3\,^2\Pi$ states are largely responsible for predissociation of the $A\,^2\Pi$ state, while other calculations indicate that the $1\,^2\Delta$ and $1\,^2\Sigma^+$ states play an important role. Nevertheless, both of these theoretical models reveal some significant discrepancies with experiment. Finally, recent measurements of the v'-dependent fine structure branching ratios have shown that exit channel coupling must be taken into account to accurately model the ClO predissociation dynamics. These results clearly indicate that more sophisticated quantum dynamical calculations are needed to fully elucidate the v'-dependent predissociation mechanism.

Bibliography

[1] M. J. Molina and F. S. Rowland, Nature **249**, 810 (1974).

[2] R. S. Stolarski and R. J. Cicerone, J. Can. Chem. **52**, 1610 (1974).

[3] J. G. Anderson, D. W. Toohey, and W. H. Brune, Science **251**, 39 (1991).

[4] Y. L. Yung, J. P. Pinto, R. T. Watson, and S. P. Sander, J. Atmos. Sci. **37**, 339 (1980).

[5] P. O. Wennberg, R. C. Cohen, R. M. Stimpfle, J. P. Koplow, J. G. Anderson, R. J. Salawitch, D. W. Fahey, E. L. Woodbridge, E. R. Keim, R. S. Gao, *et al.*, Science **266**, 398 (1994).

[6] S. R. Langhoff, L. Jaffe, and J. O. Arnold, J. Quant. Spectrosc. Radiat. Transf. **18**, 227 (1977).

[7] C. M. Nelson, T. A. Moore, M. Okumura, and T. K. Minton, J. Chem. Phys. **100**, 8055 (1994).

[8] C. M. Nelson, T. A. Moore, M. Okumura, and T. K. Minton, Chem. Phys. **207**, 287 (1996).

[9] P. Zou, J. Park, B. A. Schmitz, T. Nguyen, and S. W. North, J. Phys. Chem. A **106**, 1004 (2002).

[10] R. Schinke, *Photodissociation Dynamics* (Cambridge University Press, Cambridge, 1993).

[11] G. Pannetier and A. G. Gaydon, Nature **161**, 242 (1948).

[12] R. G. W. Norrish and G. Porter, Nature **164**, 658 (1949).

[13] G. Porter, Proc. R. Soc. Lon. Ser. A **200**, 284 (1950).

[14] G. Porter, Discuss. Faraday Soc. **9**, 60 (1950).

[15] R. A. Durie and D. A. Ramsay, Can. J. Phys. **36**, 35 (1958).

[16] J. A. Coxon, J. Photochem. **5**, 337 (1976).

[17] J. A. Coxon and D. A. Ramsay, Can. J. Phys. **54**, 1034 (1976).

[18] J. A. Coxon, J. Photochem. **6**, 439 (1977).

[19] W. H. Howie, I. C. Lane, S. M. Newman, D. A. Johnson, and A. J. Orr-Ewing, Phys. Chem. Chem. Phys. **1**, 3079 (1999).

[20] M. Mandelman and R. Nicholls, J. Quant. Spectrosc. Radiat. Transf. **17**, 483 (1977).

[21] S. A. Barton, J. A. Coxon, and U. K. Roychowdhury, Can. J. Phys. **62**, 474 (1984).

[22] M. Trolier, R. L. Mauldin III, and A. R. Ravishankara, J. Phys. Chem. **94**, 4896 (1990).

[23] P. W. McLoughlin, C. R. Park, and J. R. Wiesenfeld, J. Mol. Spectrosc. **162**, 307 (1993).

[24] G. Porter, Nobel lecture (1967). See also: http://www.nobelprize.org.

[25] I. C. Lane, W. H. Howie, and A. J. Orr-Ewing, Phys. Chem. Chem. Phys. **1**, 3087 (1999).

[26] A. Toniolo, M. Persico, and D. Pitea, J. Chem. Phys. **112**, 2790 (2000).

[27] T. Amano, S. Saito, E. Hirota, and Y. Morino, J. Mol. Spectrosc. **30**, 275 (1969).

[28] H. F. Davis and Y. T. Lee, J. Phys. Chem. **100**, 30 (1996).

[29] P. Zou, H. Kim, and S. W. North, J. Chem. Phys. **116**, 4176 (2002).

[30] H. Kim, J. Park, T. C. Niday, and S. W. North, J. Chem. Phys. **123**, 174303 (2005).

[31] D. H. A. ter Steege, M. Smits, C. A. de Lange, N. P. C. Westwood, J. B. Peel, and L. Visscher, Faraday Discuss. **115**, 259 (2000).

[32] N. Basco and R. D. Morse, J. Mol. Spectrosc. **45**, 35 (1973).

[33] Y. Matsumi, S. M. Shamsuddin, and M. Kawasaki, J. Chem. Phys. **101**, 8262 (1994).

[34] M. T. Duignan and J. W. Hudgens, J. Chem. Phys. **82**, 4426 (1985).

[35] E. Rühl, A. Jefferson, and V. Vaida, J. Phys. Chem. **94**, 2990 (1990).

[36] E. Bishenden and D. J. Donaldson, J. Chem. Phys. **99**, 3129 (1993).

[37] N. P. L. Wales, W. J. Buma, and C. A. de Lange, Chem. Phys. Lett. **259**, 213 (1996).

[38] M. J. Cooper, T. Diez-Rojo, L. J. Rogers, C. M. Western, M. N. R. Ashfold, and J. W. Hudgens, Chem. Phys. Lett. **272**, 232 (1997).

[39] J. A. Coxon, Can. J. Phys. **57**, 1538 (1979).

[40] K. Wang and V. McKoy, J. Phys. Chem. **99**, 1727 (1995).

[41] I. C. Lane and A. J. Orr-Ewing, Mol. Phys. **98**, 793 (2000).

[42] J. B. Nee and K. J. Hsu, J. Photochem. Photobiol. A **55**, 269 (1991).

[43] S. Schmidt, T. Benter, and R. N. Schindler, Chem. Phys. Lett. **282**, 292 (1998).

[44] R. Flesch, J. Plenge, S. Kühl, M. Klusmann, and E. Rühl, J. Chem. Phys. **117**, 9663 (2002).

[45] P. R. Bunker and P. C. Klein, Chem. Phys. Lett. **78**, 552 (1981).

[46] H. Kim, K. S. Dooley, G. C. Groenenboom, and S. W. North, Phys. Chem. Chem. Phys. **8**, 2964 (2006).